Progress In Electromagnetics Research Letters, Vol. 93, 107–114, 2020

A Novel Single Layer Ultra-Wideband Metamaterial Absorber

Pegah Nochian* and Zahra Atlasbaf

Abstract—Electromagnetic interference (EMI) is a crucial problem, and for solving this problem, absorbers especially very thin absorbers are used. Factors like frequency increasing in a device, high integration in electronic systems, higher power densities, and decreasing the size and thickness of PCB make it crucial. So, a novel ultra-wideband and thin metamaterial absorber is proposed in this paper. The absorber consists of metamaterial unit cells, which have a single FR4† layer, metallic ground, and four metallic spirals. A one hundred ohms SMD‡ resistor is placed between two of the spirals. The size of the unit cell is $5.85 \times 5.85 \times 3.2\,\mathrm{mm}^3$. The proposed absorber is ultra-thin ($\lambda_0/10$), and the absorption occurs over a wide incident angle [0°–40°]. The reflection is less than -12 dB in [6.5 GHz–12 GHz], and the absorption is more than 94% in this bandwidth. The structure is fabricated, and the outcomes of simulation and measurement are compared with each other. The values of front to back ratio of the fabricated measurements are -12.8, -7.31, and -15.36 dB at 8, 10, and 12 GHz, respectively. The values obtained from simulation are -13, -9.4 and -14 dB, respectively. There is a good agreement (accordance) between the simulation and measurement results of this absorber.

1. INTRODUCTION

Electromagnetic interference (EMI) is an important problem since it can happen anyplace in electronic circuits with unpredictable and damaging effects. One of the solutions for this problem is using absorbers, especially very thin absorbers. Therefore, absorbers like Salisbury screen [1] and Jauman absorber [2] were used in earlier days. Salisbury absorbers consist of a resistive sheet placed $\lambda/4$ in front of the perfectly conducting plane, and for making wider bandwidth Jauman absorber was designed. It has two resistive screens and a groundsheet placed $\lambda/4$ from each other.

Another kind of absorbers is a frequency selective surface. In some instances, the Frequency Selective Surfaces (FSSs) are loaded by the lumped resistors [3–5], while in some structures, the FSSs are made with resistive sheet [6, 7].

The important factors of designing an absorber are lightening and thinning that can be achieved by using metamaterial structures since metamaterials are thin [8] and small. In 2008, Landy et al. [9] designed a metamaterial absorber for the first time.

The most significant challenge is designing a broadband metamaterial absorber since metamaterials are inherently narrow-band. Many previous works, such as single band [10], dual-band, and multi-band [11–13], are narrow-band at each operating frequency. The metamaterial absorbers can be made over different frequency bands including microwave [14], terahertz (THz) [15], near-infrared, and optical regimes [16]. A remarkable method is utilizing lumped elements to achieve broadband absorption [17–20]. Most of the works that have symmetric structures are almost polarization-independent, like the absorber reported in [21].

Received 14 January 2020, Accepted 3 September 2020, Scheduled 28 September 2020
* Corresponding author: Pegah Nochian (pegah.nochian@yahoo.com).
The authors are with the Department of Electrical & Computer Engineering, Tarbiat Modars University, Tehran, Iran.
† Flame Retardant 4.
‡ Surface Mount Device.

In this article, a novel ultra-wideband metamaterial absorber is introduced. In Section 2, the principle of metamaterial absorber is discussed. The design of an absorber is illustrated, and the outcomes are studied in Section 3. By investigating the obtained results, it can be seen that up to 40 degrees absorption variation is only a little, and it is due to the almost symmetric structure of the proposed absorber. Reflection and absorption diagrams are plotted for different incident angles (up to 40 degrees) while surface current is studied under different frequencies. Finally, the fabrication and measurement procedures are discussed in Section 4.

2. PRINCIPLE OF METAMATERIAL ABSORBER

It is well known that the absorption is defined as: $1 - |S_{11}|^2 - |S_{21}|^2$, where S_{11} is the reflection coefficient, and S_{21} is the transmission coefficient. Transmission is about zero since the bottom layer is metallic. Thus, the absorption can be obtained by minimizing the reflection of the absorber structure. For obtaining the minimum reflection, the impedance of the absorber must be matched to free space impedance. To design a broadband perfect metamaterial absorber, the parameters of the unit cell must be carefully optimized to make sure that absorber's impedance is equal to the impedance of free space approximately at the whole of absorption frequency band. It means that S_{11} is almost zero. Another equation for checking impedance matching is

$$Z_M(\omega) = \sqrt{\mu_r(\omega)/\varepsilon_r(\omega)} \tag{1}$$

where Z_M is the normalized impedance of the absorber. For impedance matching, relative permeability ($\mu_r(\omega)$) and relative permittivity ($\varepsilon_r(\omega)$) should be equal, and it makes $Z(\omega)$ unity.

Metamaterials can be characterized by their complex relative permittivity $\varepsilon_r(\omega) = \varepsilon_1 + \mathrm{i}\varepsilon_2$ and relative permeability $\mu_r(\omega) = \mu_1 + \mathrm{i}\mu_2$. Thus, by designing a proper unit cell of the absorber and optimizing all of its parameters, $\mu_1(\omega)$ or $\varepsilon_1(\omega)$ can become negative values. Therefore, the loss can be increased because β which is mentioned in Eq. (2) is imaginary.

$$\beta = \frac{\omega}{c}\sqrt{\mu_r(\omega)\varepsilon_r(\omega)} \tag{2}$$

The simulated relative permittivity and permeability of the proposed unit cell (Fig. 4) are shown in Figs. 1 to 3. As can be seen in Fig. 1, the relative permittivity has a positive real component in some parts of the frequency band and negative in other parts. In the frequency part that the real component of permittivity is negative, the real component of permeability is positive and vice versa. The imaginary component of the relative permittivity and the relative permeability is positive all over the frequency bandwidth as noted in Fig. 2. It should be pointed out that these diagrams are obtained from Equations (3) to (6) [22] by a commercial software (CST). $\mu_r(\omega) \cdot \varepsilon_r(\omega)$ is negative all over the bandwidth as seen in Fig. 3. It causes β imaginary for the whole bandwidth (Fig. 3). These features

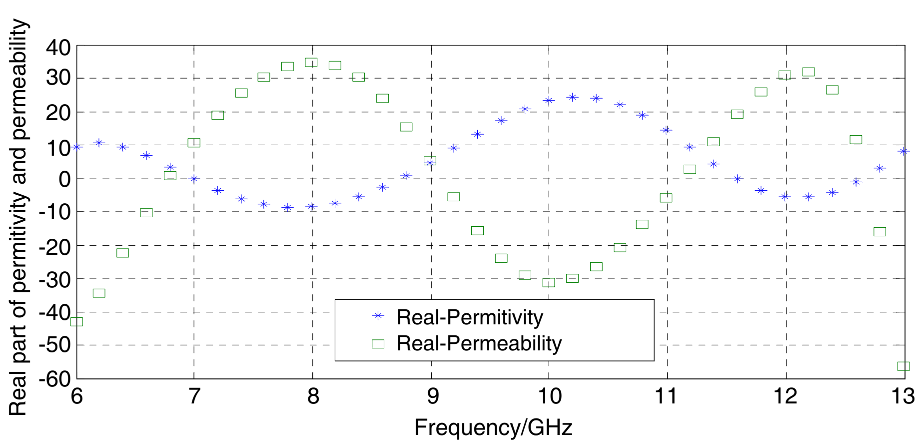

Figure 1. Real component of relative permittivity and relative permeability.

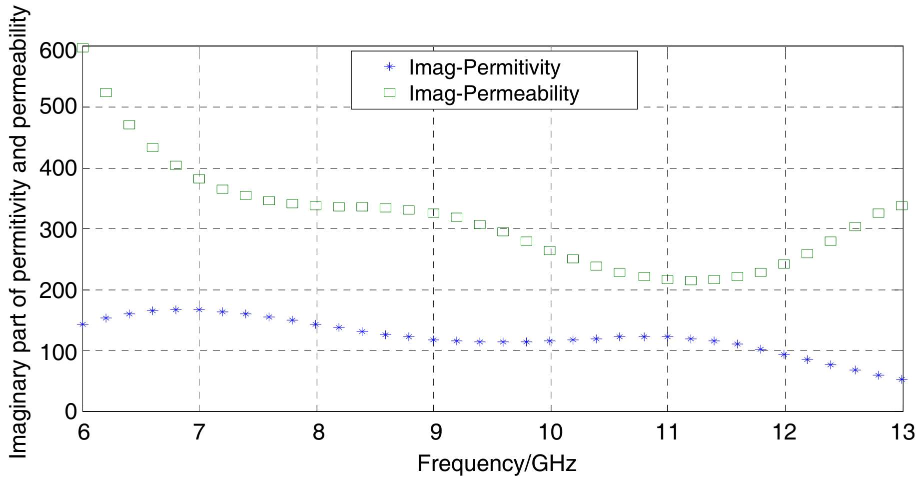

Figure 2. Imaginary component of permittivity and permeability.

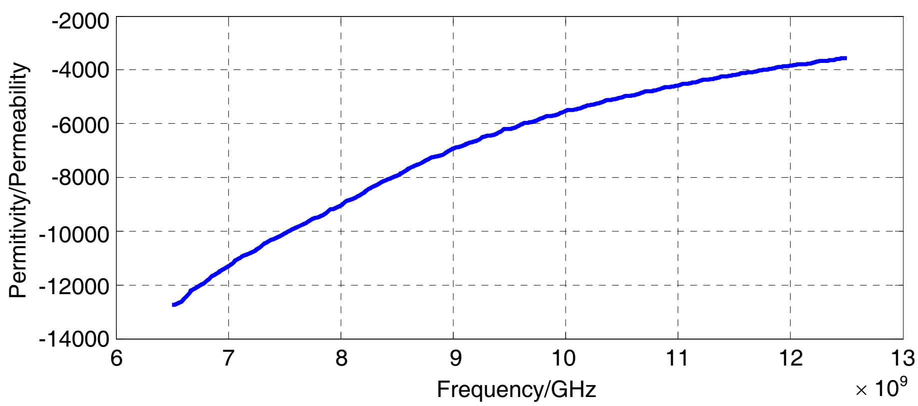

Figure 3. Plot of $\mu_{eff}(\omega) \times \varepsilon_{eff}(\omega)$.

cause a loss in the absorber [21].

$$z = \sqrt{\frac{(1+s_{11}^2)-s_{21}^2}{(1-s_{11}^2)-s_{21}^2}} \tag{3}$$

$$n = \frac{1}{kd}\cos^{-1}\left[\frac{1}{2S_{21}}\left(1-S_{11}^2+S_{21}^2\right)\right] \tag{4}$$

$$\mu = nz \tag{5}$$

$$\varepsilon = n/z \tag{6}$$

Under oblique incident angle, reflection is not zero. The reflection coefficient of the transverse electric (TE) mode is [22]:

$$\Gamma_{\perp}(\omega) = \frac{Z_M(\omega)\cos\theta_i - Z_0\cos\theta_t}{Z_M(\omega)\cos\theta_i + Z_0\cos\theta_t} \tag{7}$$

where θ_i, θ_t are the incident and transmitted angles, respectively, and Z_0 is the free space impedance. For the transverse magnetic (TM), the reflection coefficient is as follows [22]:

$$\Gamma_{\text{II}}(\omega) = \frac{Z_M(\omega)\cos\theta_t - Z_0\cos\theta_i}{Z_M(\omega)\cos\theta_t - Z_0\cos\theta_i} \tag{8}$$

In general, metamaterial absorbers are allocated to meet a zero-reflection condition when the incidence wave is normal. Since the reflection coefficient is not zero under oblique incidence, the absorption factor of a metamaterial absorber is reduced as the incident angle is raised. In order to solve this problem, an incident angle almost-insensitive unit cell is proposed for metamaterial absorbers in this article.

3. DESIGN AND SIMULATION RESULTS

Figure 4 shows the geometry of the introduced ultra-wideband absorber. The optimized dimensions of the presented unit cell are shown in this picture. The single unit cell consists of a metallic patch on top, and bottom ground plane below the dielectric substrate.

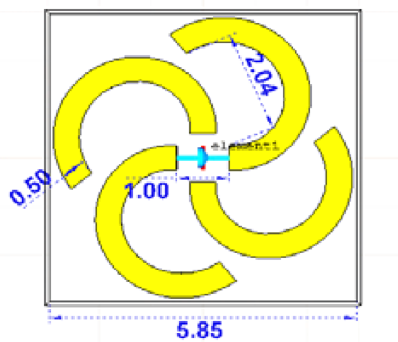

Figure 4. The structure of the absorber (all dimensions are in mm).

FR4-substrate (relative permittivity $\varepsilon_r = 4.3$ and dielectric loss tangent $\tan\delta = 0.025$) has been used as the dielectric with a thickness of 3.2 mm. The top layer consists of four single spirals and one 100 ohm resistor. The size of the unit cell is $5.85 \times 5.85 \times 3.2\,\text{mm}^3$. Both the top patch and bottom ground are built of copper with the thickness of 0.035 mm. The unit cell is designed with periodic boundary condition by using CST 2017.

In the entire [6.5 GHz–12 GHz] S_{11} is better than -12 dB at the normal incident wave. Up to 40 degrees of the incident angle S_{11} is better than -9.8 dB, and there is also a little shift since the structure is not totally symmetric. The two peaks are also visible at 7.49 and 11.09 GHz as demonstrated in Fig. 5.

In the entire X-band (6.5 GHz–12 GHz), the absorption is above 94% at the normal incident wave (0 degrees of the incident angle). As mentioned before, the absorptivity is $1 - |S_{11}|^2 - |S_{21}|^2$, and it

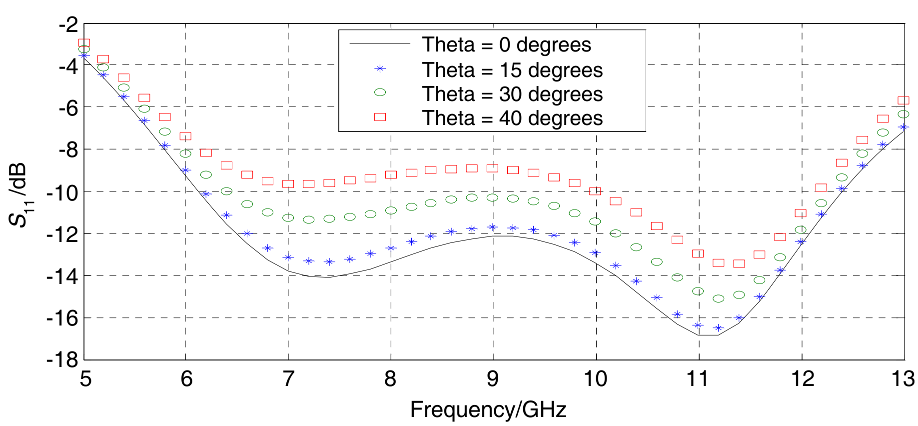

Figure 5. Reflection in different incident angle.

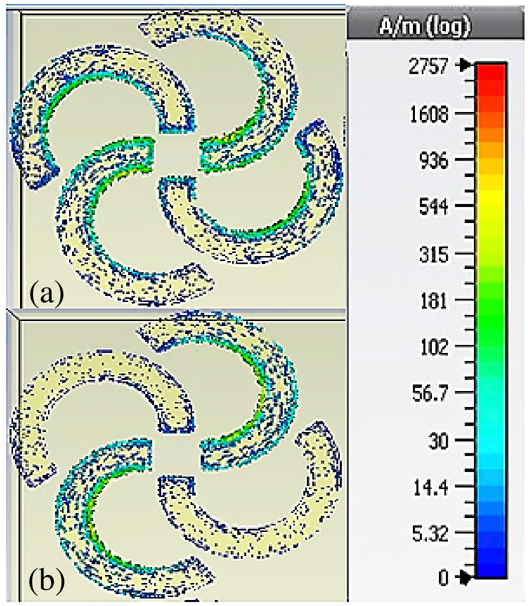

Figure 6. Surface current (a) 7.49 GHz, (b) 11.09 GHz.

can be seen in Fig. 5 that S_{11} (reflection) is less than -12 dB. Because of the metallic backplane, the transmission is almost zero. So, the absorption is almost unity.

As can be seen in Fig. 6, at upper-frequency, the surface current is more distributed around two spirals, but at lower frequency surface current is distributed on four spirals.

4. FABRICATION

In order to experimentally illustrate the proposed absorber, a sheet consisting of $37 * 37$ unit cells has been fabricated on a 2 mm thick metallic back FR4 as noted in Fig. 7.

To measure F/B ratio, a horn antenna is used which is a linearly polarized antenna, and it radiates to the front of the absorber. Then, the reflected pattern and radiation to the back of the absorber are

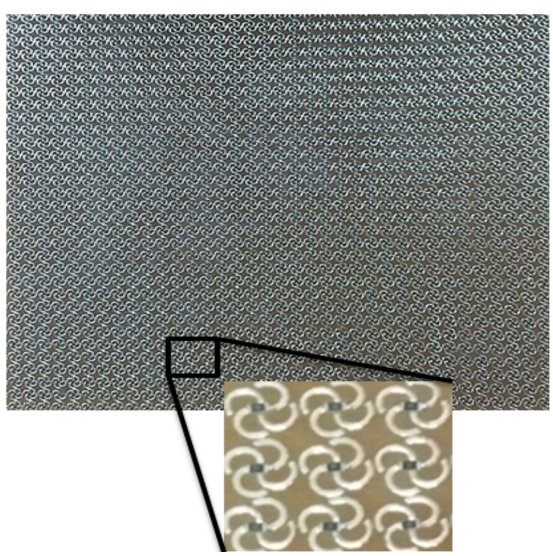

Figure 7. Fabricated structure (on FR4 with $\varepsilon_r = 4.3$, $\tan\delta = 0.025$).

measured. The difference between these two measurements (in dB) is called F/B (Front to Back Ratio).

Front to back ratio is measured from the fabricated structure and simulated as shown in Fig. 8. Its values of the fabricated measurements are -12.8, -7.31 and -15.36 dB in 8, 10, and 12 GHz, respectively. The values obtained from simulation are -13, -9.4 and -14 dB, respectively. There are some differences between simulation and measurement results for some fabrication and measurement errors.

In Fig. 9, the front to back ratio of the fabricated absorber is shown in three frequencies. Its

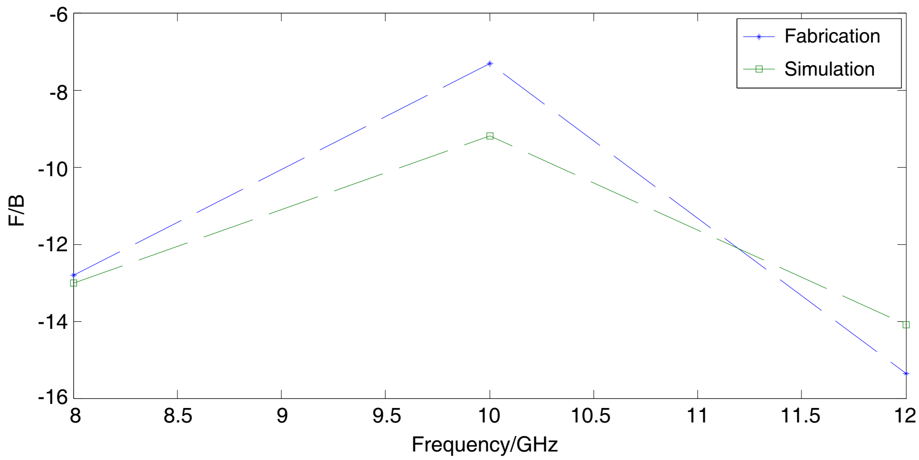

Figure 8. Front to back ratio of the fabricated and simulated structure.

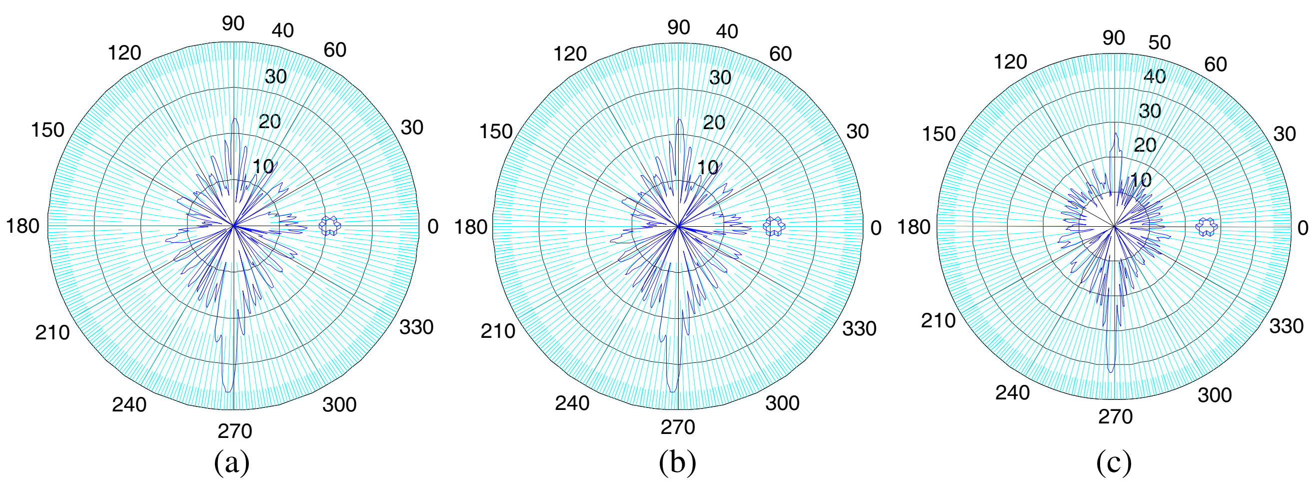

Figure 9. Measured return pattern from absorber in (a) 8 GHz, (b) 10 GHz, (c) 12 GHz.

Table 1. Absorption comparison.

	Bandwidth (-10 dB)	Theta independent	Thickness	Number of layer
[17]	61.7	yes	4.2 mm	3
[19]	10.2%	No	3.2 mm	1
[16]	129.7%	Not mentioned	14 nm	2
[18]	40%	No	3 mm	1
Our Work	68%	Yes	3.2 mm	1

values for measurements of fabricated absorber are −12.8, −7.31, and −15.36 dB at 8, 10, and 12 GHz, respectively.

The pattern of horn antenna has hit the absorber, and reflected pattern has been calculated. For each frequency, the absorber has been rotated from 0 to 360 degrees, and the horn pattern has hit the absorber in different rotation angles.

As mentioned in Table 1, the new structure has an ultra-wideband compared to the other structures. In addition, the independent incident angle is up to 40 degrees.

5. CONCLUSION

In this article, a novel ultra-broadband metamaterial absorber has been designed. The principle of a metamaterial absorber has been discussed. The absorber was designed, and the outcomes were studied. Finally, the fabrication and measurement process were discussed. The new structure has ultra-wideband compared to the other structures as mentioned in Table 1. In addition, the independent incident angle is up to 40 degrees.

ACKNOWLEDGMENT

The authors would like to thank Abootorab at the Antenna Lab of K. N. Toosi University of Technology for the measurements.

REFERENCES

1. Fante, R. L. and M. T. McCormack, "Reflection properties of the Salisbury screen," *IEEE Transactions on Antennas and Propagation*, Vol. 36, 1443–1454, 1988.
2. Du Toit, L. J., "The design of Jauman absorbers," *IEEE Antennas and Propagation Magazine*, Vol. 36, 17–25, 1994.
3. Yang, J. and Z. Shen, "A thin and broadband absorber using double-square loops," *IEEE Antennas and Wireless Propagation Letters*, Vol. 6, 388–391, 2007.
4. Tang, W. and Z. Shen, "Simple design of thin and wideband circuit analogue absorber," *Electronics Letters*, Vol. 43, 689–691, 2007.
5. Seman, F. C., R. Cahill, V. Fusco, and G. Goussetis, "Design of a Salisbury screen absorber using frequency selective surfaces to improve bandwidth and angular stability performance," *IET Microwaves, Antennas & Propagation*, Vol. 5, 149–156, 2011.
6. Costa, F., A. Monorchio, and G. Manara, "Analysis and design of ultra thin electromagnetic absorbers comprising resistively loaded high impedance surfaces," *IEEE Transactions on Antennas and Propagation*, Vol. 58, 1551–1558, 2010.
7. Luukkonen, O., F. Costa, C. R. Simovski, A. Monorchio, and S. A. Tretyakov, "A thin electromagnetic absorber for wide incidence angles and both polarizations," *IEEE Transactions on Antennas and Propagation*, Vol. 57, 3119–3125, 2009.
8. El-Aasser, M. A., "Design optimization of nanostrip metamaterial perfect absorbers," *Journal of Nanophotonics*, Vol. 8, 083085, 2014.
9. Landy, N. I., S. Sajuyigbe, J. Mock, D. Smith, and W. Padilla, "Perfect metamaterial absorber," *Physical Review Letters*, Vol. 100, 207402, 2008.
10. Fallahzadeh, S., K. Forooraghi, and Z. Atlasbaf, "Design, simulation and measurement of a dual linear polarization insensitive planar resonant metamaterial absorber," *Progress In Electromagnetics Research Letters*, Vol. 35, 135–144, 2012.
11. Bian, B., S. Liu, S. Wang, X. Kong, H. Zhang, B. Ma, et al., "Novel triple-band polarization-insensitive wide-angle ultra-thin microwave metamaterial absorber," *Journal of Applied Physics*, Vol. 114, 194511, 2013.
12. Shen, X., T. J. Cui, J. Zhao, H. F. Ma, W. X. Jiang, and H. Li, "Polarization-independent wide-angle triple-band metamaterial absorber," *Optics Express*, Vol. 19, 9401–9407, 2011.

13. Cheng, Y., M. Huang, H. Chen, Z. Guo, X. Mao, and R. Gong, "Ultrathin six-band polarization-insensitive perfect metamaterial absorber based on a cross-cave patch resonator for terahertz waves," *Materials*, Vol. 10, 591, 2017.
14. Mahmood, A., G. Ögücü Yetkin, and C. Sabah, "Design and fabrication of a novel wideband DNG metamaterial with the absorber application in microwave X-band," *Advances in Condensed Matter Physics*, Vol. 2017, 2017.
15. Tao, H., C. Bingham, D. Pilon, K. Fan, A. Strikwerda, D. Shrekenhamer, et al., "A dual band terahertz metamaterial absorber," *Journal of Physics D: Applied Physics*, Vol. 43, 225102, 2010.
16. Hao, J., J. Wang, X. Liu, W. J. Padilla, L. Zhou, and M. Qiu, "High performance optical absorber based on a plasmonic metamaterial," *Applied Physics Letters*, Vol. 96, 251104, 2010.
17. Shang, Y., Z. Shen, and S. Xiao, "On the design of single-layer circuit analog absorber using double-square-loop array," *IEEE Transactions on Antennas and Propagation*, Vol. 61, 6022–6029, 2013.
18. Yoo, M. and S. Lim, "Polarization-independent and ultrawideband metamaterial absorber using a hexagonal artificial impedance surface and a resistor-capacitor layer," *IEEE Transactions on Antennas and Propagation*, Vol. 62, 2652–2658, 2014.
19. Sohrab, A. P. and Z. Atlasbaf, "A circuit analog absorber with optimum thickness and response in X-band," *IEEE Antennas and Wireless Propagation Letters*, Vol. 12, 276–279, 2013.
20. Lee, D., H. Jeong, and S. Lim, "Electronically switchable broadband metamaterial absorber," *Scientific Reports*, Vol. 7, 4891, 2017.
21. Li, H., L. H. Yuan, B. Zhou, X. P. Shen, Q. Cheng, and T. J. Cui, "Ultrathin multiband gigahertz metamaterial absorbers," *Journal of Applied Physics*, Vol. 110, 014909, 2011.
22. Numan, A. B. and M. S. Sharawi, "Extraction of material parameters for metamaterials using a full-wave simulator [education column]," *IEEE Antennas and Propagation Magazine*, Vol. 55, 202–211, 2013.